Proceedings of International Conference on Power System Transients
Rio de Janeiro - RJ - Brazil - June 2001

Detailed Model of Long Transmission Lines for Modal Analysis of ac Networks

Sergio Gomes Jr.[1,2] Carlos Portela[2] Nelson Martins[1]

[1]CEPEL - Caixa Postal 68.007, 21944-970, Rio de Janeiro, RJ, Brazil
[2]COPPE/UFRJ - Caixa Postal 68.564, 21945-970, Rio de Janeiro, RJ, Brazil
e-mails: sgomes@cepel.br / portela@coep.ufrj.br / nelson@cepel.br

Abstract: This paper describes a detailed s-domain model for long transmission lines to be used in the modal analysis of ac networks. Structural information on the system may be obtained with modal analysis, which nicely complement those obtained by the traditional time and frequency response analyses. The s-domain model considers the distributed parameters of the transmission lines and also their frequency dependency, taking into account the skin effect and ground return path influence. Modal analysis results are included.

Keywords: Transmission Lines, Skin Effect, Ground Return, Modal Analysis, s-Domain, ac Networks.

I. INTRODUCTION

Networks containing detailed transmission line models can be analyzed using different approaches such as time domain simulation [1,2,3] and frequency scan [2,3].

Additional information on the system may be obtained from modal analysis, which complement those obtained by the traditional time and frequency response techniques. This is system structural information, such as series and parallel resonances and their sensitivities to parameter changes. Reduced order linear models for the system may also be obtained with the use of modal analysis.

Modal analysis of ac networks, incorporating the RLC transients, is traditionally carried out using state space models [4]. Recent papers [5] have proposed using the descriptor systems approach to model ac networks, which automatically deals with state variable redundancies and leads to more efficient computer implementations. Both approaches have to use approximations based on ladder circuits or Padé polynomials when modeling long transmission lines, which usually cause severe problems.

The modeling of frequency dependent transmission lines in ac networks for modal analysis is best carried out in the s-domain. The ac network may be modeled as a nodal admittance matrix in the s-domain, $\mathbf{Y}(s)$, as described in [6]. Robust and efficient eigensolution algorithms specially suited to the $\mathbf{Y}(s)$ model are developed in [7]. These algorithms require the determination of the $\mathbf{Y}(s)$ derivatives with respect to s.

This paper describes a detailed transmission line model that may be used for the modal analysis of ac networks represented in the s-domain. The frequency dependency of transmission line parameters is considered, including the conductor skin effect and the ground return path. Modal analysis results are presented for the described line model.

II. S-DOMAIN MODEL

The ac network dynamic equations may be assembled as a nodal admittance matrix in the s-domain, $\mathbf{Y}(s)$. Each diagonal element of this matrix is equal to the sum of the operational admittances (functions of s) of all the elements connected to a given node. The off-diagonal elements are equal to the negative value of the sum of the operational admittances of the branches connecting the corresponding nodes. This matrix must be reassembled for each complex frequency of interest. The following equation is formed for a general ac network [6,7]:

$$\mathbf{Y}(s)\cdot\mathbf{v}=\mathbf{i} \tag{1}$$

where $\mathbf{Y}(s)$ is the system nodal admittance matrix in the s-domain, $\mathbf{v}$ the vector of bus voltages and $\mathbf{i}$ the vector of injected currents.

Equation (1) may be particularized for single-input-single-output systems, as presented in (2), where the input variable i_k is the injected current in bus k while the output variable v_j is the voltage at bus j . Vector $\mathbf{b}$ is comprised of zero elements except for the k-th element that has a unity value. The row vector $\mathbf{c}$ is also comprised of zeros except for the j-th element, which is equal to unity:

$$\begin{aligned}\mathbf{Y}(s)\cdot\mathbf{v}&=\mathbf{b}\cdot i_k\\ v_j&=\mathbf{c}\cdot\mathbf{v}\end{aligned} \tag{2}$$

One should note that the number of system states is, in general, considerably larger than the dimension of matrix $\mathbf{Y}(s)$. This is due to the fact that every system element connected to a node of $\mathbf{Y}(s)$ is a second or higher order operational admittance (RLC branches) or analytical functions in s which describe the dynamics of the transmission lines.

As an example, a RLC branch has the following operational admittance:

$$y=\frac{1}{R+s\cdot L+\dfrac{1}{s\cdot C}} \tag{3}$$

Assuming this RLC branch connects nodes i and j, the above elements must be added to the diagonals (i,i) and (j,j) of $\mathbf{Y}(s)$. The same elements must be added, with negative signs, to the off-diagonal elements (i,j) and (j,i).

The eigensolution methods proposed in [7] require the calculation of the derivative of $\mathbf{Y}(s)$ with respect to s. The derivative of $\mathbf{Y}(s)$ is built following the same logic used to assemble $\mathbf{Y}(s)$, with the difference that the derivatives of the operational admittances of the branches are now used.

The derivative of the RLC branch admittance is:

$$\frac{dy}{ds}=\frac{-L+\dfrac{1}{s^2C}}{\left(R+s\cdot L+\dfrac{1}{s\cdot C}\right)^2} \tag{4}$$

III. MODAL ANALYSIS FOR S-DOMAIN MODELS

Manipulation of the two equations in (2) yields the relationship between the system input (v_j) and output (i_k) variables, also known as the transfer function $G(s)$:

$$G(s) = \frac{y}{u} = \mathbf{c} \cdot \left[\mathbf{Y}(s) \right]^{-1} \cdot \mathbf{b} \tag{5}$$

Substituting s for $j\,\omega$, one obtains the network harmonic impedance $G(j\,\omega)$, which is used to calculate the frequency scan of the system. These methods based on the building of $\mathbf{Y}(j\,\omega)$, for a set of discrete values of ω are widely used in harmonic analysis programs. The s-domain modeling is more general because it uses the complex variable s, instead of the purely imaginary $j\,\omega$. The s-domain approach allows the modal analysis of the system [7].

The time response of y to an impulse disturbance applied in u is equal to the inverse Laplace transform of $G(s)$, considering zero initial conditions in all system states. This time response will be of the form:

$$y = \sum_i R_i \cdot e^{\lambda_i \cdot t} \tag{6}$$

where λ_i are the poles of $G(s)$ and R_i their associated residues. The poles of $G(s)$ are those values of s that produce singularity in $G(s)$. Every pole of $G(s)$ causes the matrix $\mathbf{Y}(s)$ to become singular ($\det[\mathbf{Y}(s)] = 0$), and therefore not inversible. Any chosen transfer function has the same set of poles, since they are completely defined by the matrix $\mathbf{Y}(s)$.

The s-domain algorithm for the calculation of the dominant poles of a transfer function is given below [7]:

$$\begin{bmatrix} \mathbf{Y}\left(\lambda^{(k)}\right) & -\mathbf{b} \\ \mathbf{c} & 0 \end{bmatrix} \cdot \begin{bmatrix} \mathbf{v}^{(k)} \\ u^{(k)} \end{bmatrix} = \begin{bmatrix} \mathbf{0} \\ 1 \end{bmatrix} \tag{7}$$

$$\begin{bmatrix} \mathbf{Y}\left(\lambda^{(k)}\right)^t & \mathbf{c}^t \\ -\mathbf{b}^t & 0 \end{bmatrix} \cdot \begin{bmatrix} \mathbf{w}^{(k)} \\ u^{(k)} \end{bmatrix} = \begin{bmatrix} \mathbf{0} \\ 1 \end{bmatrix} \tag{8}$$

$$\Delta\lambda^{(k)} = \frac{u^{(k)}}{\left[\mathbf{w}^{(k)}\right]^t \cdot \dfrac{d\mathbf{Y}\left(\lambda^{(k)}\right)}{ds} \cdot \mathbf{v}^{(k)}} \tag{9}$$

After choosing an estimate $\lambda^{(0)}$ for the pole, one should build the matrix $\mathbf{Y}(\lambda^{(0)})$ and its derivative with respect to s and solve the linear systems (7) and (8), obtaining the vectors $\mathbf{v}$ and $\mathbf{w}$ and scalar u for the first iteration. The correction $\Delta\lambda$ may then be calculated using (9) as a function of u, $\mathbf{v}$, $\mathbf{w}$ and the derivative of the matrix $\mathbf{Y}(s)$. The updated value of λ is given by:

$$\lambda^{(k+1)} = \lambda^{(k)} + \Delta\lambda^{(k)} \tag{10}$$

This procedure is iterated until the modulus of the increment $\Delta\lambda$ becomes smaller than a specified tolerance. The approximation for the transfer function residue at the $(k + 1)$ iteration, associated with the pole λ is given by [7]:

$$R_i^{(k+1)} = -\frac{1}{\left[\mathbf{w}^{(k)}\right]^t \cdot \dfrac{d\mathbf{Y}\left(\lambda^{(k)}\right)}{ds} \cdot \mathbf{v}^{(k)}} \tag{11}$$

Once the pole is converged, the expression (11) provides an accurate value for the residue.

IV. DISTRIBUTED PARAMETER TRANSMISSION LINE MODELING

The single-phase or single-mode model of a transmission line has the following admittances [8]:

$$y_s = y_c \cdot \coth(\gamma \cdot l) \tag{12}$$

$$y_m = y_c \cdot \operatorname{csch}(\gamma \cdot l) \tag{13}$$

where y_s is the admittance to be added to the diagonals of $\mathbf{Y}(s)$ while y_m is the admittance to be added to the off-diagonal terms, with negative sign. The line admittances are functions of its length l, the propagation constant γ and the characteristic admittance y_c. The constants γ and y_c shown in (14) are functions of the line parameters per unit length: longitudinal impedance per unit length, Z_u , and transversal admittance per unit length, Y_u , which depend on s.

$$\gamma = \sqrt{Z_u(s) \cdot Y_u(s)} \qquad y_c = \sqrt{\frac{Y_u(s)}{Z_u(s)}} \tag{14}$$

The derivatives of the line admittances with respect to s are given by:

$$\frac{dy_s}{ds} = \frac{dy_c}{ds} \cdot \coth(\gamma\, l) - y_c \cdot \frac{d\gamma}{ds} \cdot l \cdot \operatorname{csch}(\gamma\, l) \tag{15}$$

$$\frac{dy_m}{ds} = \frac{dy_c}{ds} \cdot \operatorname{csch}(\gamma\, l) - y_c \cdot \frac{d\gamma}{ds} \cdot l \cdot \operatorname{csch}(\gamma\, l) \cdot \coth(\gamma\, l) \tag{16}$$

where

$$\frac{dy_c}{ds} = \frac{1}{2 \cdot \sqrt{Z_u \cdot Y_u}} \cdot \left[\frac{dY_u}{ds} - y_c^{\,2} \cdot \frac{dZ_u}{ds} \right] \tag{17}$$

$$\frac{d\gamma}{ds} = \frac{1}{2\gamma} \left[Z_u \cdot \frac{dY_u}{ds} + Y_u \cdot \frac{dZ_u}{ds} \right] \tag{18}$$

Some of the advantages of using the s-domain representation include the fact that there is no need to define the network state variables or to derive the dynamic equations for the various system elements as a function of the states. Note also that, in the case of the distributed-parameter transmission line there is an infinite number of states, due to the inherent characteristics of the hyperbolic functions in the line model. Approximate, finite-order, state space or descriptor system models exist for the distributed-parameter transmission line, using ladder networks or polynomial approximations of the Padé type [9]. However, as one attempts to improve the model's accuracy by increasing the model order, there appears numerical problems, extremely large system models and extraneous results, as demonstrated in [10]. The s-domain model, on the other hand, does not present any of these three disadvantages.

V. TRANSMISSION LINE PARAMETERS

The line parameters per unit length of longitudinal impedance Z_u and transversal admittance Y_u are obtained from the reduction of the matrices $\mathbf{Z_u}$ and $\mathbf{Y_u}$ containing the parameters of the various individual line conductors [11].

The quasi-stationary approximation, which assumes the capacitance matrix $\mathbf{C}$ to be independent of s, is quite

adequate to the present application. The admittance matrix may then be expressed by:

$$\mathbf{Y_u} = s \cdot \mathbf{C} \tag{19}$$

The derivative of matrix $\mathbf{Y_u}$ with respect to s is, therefore, equal to the capacitance matrix $\mathbf{C}$.

The longitudinal impedance matrix comprises the sum of three terms:

$$\mathbf{Z_u} = \mathbf{Z^{(e)}} + \mathbf{Z^{(i)}} + \mathbf{Z^{(g)}} \tag{20}$$

The term $\mathbf{Z^{(e)}}$ corresponds to the external impedance, assuming ideal conductors and no ground losses. The term $\mathbf{Z^{(i)}}$ describes the internal conductor impedances, and $\mathbf{Z^{(g)}}$ contains the corrections needed due to the non-ideal ground return path.

The matrix $\mathbf{Z^{(e)}}$ is given by the product of s and the external inductance matrix ($\mathbf{L^{(e)}}$) which does not depend on s (the quasi-stationary approximation):

$$\mathbf{Z^{(e)}} = s \cdot \mathbf{L^{(e)}} \tag{21}$$

The derivative of the term $\mathbf{Z^{(e)}}$ with respect to s is, therefore, equal to the external inductance matrix.

The external inductance will be proportional to the inverse of the capacitance matrix, as a result of the quasi-stationary approximation:

$$\mathbf{L^{(e)}} = \mu_0 \cdot \varepsilon_0 \cdot \mathbf{C}^{-1} \tag{22}$$

where μ_0 and ε_0 are respectively the magnetic permeability and electric permittivity of the air.

The term associated with the conductor internal impedances is a diagonal matrix and a function of s. The conductor internal impedances may be modeled in two forms, either utilizing Bessel functions [12] or the complex depth concept [13].

Both formulations consider the conductors to be represented by a annular cross-section of external radius r_e and internal radius r_i , which defines the dimensions of the aluminum external part and the steel core of the ACSR conductors. It is here assumed, as in most other applications, that the current does not flow through the steel core. This turns simpler the mathematical formulation, which is described below. The internal impedance of the conductor is given by [12]:

$$z_i = k(s) \cdot \frac{n(s)}{d(s)} \tag{23}$$

where:

$$k(s) = \sqrt{\frac{s \cdot \mu_0}{\sigma}} \cdot \frac{1}{2 \cdot \pi \cdot r_e}$$

$$n(s) = I_0(\rho_1) \cdot K_1(\rho_0) + I_1(\rho_0) \cdot K_0(\rho_1)$$

$$d(s) = I_1(\rho_1) \cdot K_1(\rho_0) + I_1(\rho_0) \cdot K_1(\rho_1)$$

$$\rho_0 = r_i \cdot \sqrt{s \cdot \mu \cdot \sigma} \qquad \rho_1 = r_e \cdot \sqrt{s \cdot \mu \cdot \sigma}$$

I_0, I_1 are the modified Bessel functions of first kind while K_0 and K_1 are the modified Bessel functions of second kind. Indexes 0 and 1 represent the order of the functions. The parameter σ is the conductor conductivity and μ is the conductor magnetic permeability.

The derivative with respect to s of the internal impedance is given by:

$$\frac{dz_i}{ds} = \frac{d\,k(s)}{ds} \cdot \frac{n(s)}{d(s)} + k(s) \cdot \frac{d(s)\frac{d\,n(s)}{ds} + n(s)\frac{d\,d(s)}{ds}}{d(s)^2} \tag{24}$$

where:

$$\frac{d\,k(s)}{ds} = \frac{k(s)}{2 \cdot s}$$

$$\frac{d\,n(s)}{ds} = \frac{d\,I_0(\rho_1)}{d\,\rho_1} \cdot \frac{d\,\rho_1}{d\,s} \cdot K_1(\rho_0) + I_0(\rho_1) \cdot \frac{d\,K_1(\rho_0)}{d\rho_0} \cdot \frac{d\,\rho_0}{d\,s} + \frac{d\,I_1(\rho_0)}{d\,\rho_0} \cdot \frac{d\,\rho_0}{d\,s} \cdot K_0(\rho_1) + I_1(\rho_0) \cdot \frac{d\,K_0(\rho_1)}{d\rho_1} \cdot \frac{d\,\rho_1}{d\,s}$$

$$\frac{d\,d(s)}{ds} = \frac{d\,I_1(\rho_1)}{d\,\rho_1} \cdot \frac{d\,\rho_1}{d\,s} \cdot K_1(\rho_0) + I_1(\rho_1) \cdot \frac{d\,K_1(\rho_0)}{d\rho_0} \cdot \frac{d\,\rho_0}{d\,s} - \frac{d\,I_1(\rho_0)}{d\,\rho_0} \cdot \frac{d\,\rho_0}{d\,s} \cdot K_1(\rho_1) - I_1(\rho_0) \cdot \frac{d\,K_1(\rho_1)}{d\rho_1} \cdot \frac{d\,\rho_1}{d\,s}$$

$$\frac{d\rho_0}{ds} = \frac{\rho_0}{2 \cdot s}$$

$$\frac{d\rho_1}{ds} = \frac{\rho_1}{2 \cdot s}$$

The derivatives of the modified Bessel functions are given by:

$$\frac{dI_0(\rho)}{d\rho} = I_1(\rho)$$

$$\frac{dI_1(\rho)}{d\rho} = \frac{I_0(\rho) + I_2(\rho)}{2}$$

$$\frac{dK_0(\rho)}{d\rho} = -K_1(\rho)$$

$$\frac{dK_1(\rho)}{d\rho} = -\frac{K_0(\rho) + K_2(\rho)}{2}$$

where the indexes 0, 1 and 2 represent the order of first kind (I) or second kind (K) modified Bessel functions.

The internal impedance can alternatively be modeled using the complex depth p [13]:

$$p = \frac{1}{\sqrt{s \cdot \mu_0 \cdot \sigma}} \tag{25}$$

The internal impedance is given by [13]:

$$z_i = \sqrt{z_0 + z_\infty} \tag{26}$$

where z_0 is the conductor impedance at zero frequency and z_∞ the conductor impedance as the frequency approaches infinity. The impedance z_0 is the dc resistance, being given by:

$$z_0 = \frac{1}{\pi \left(r_e^2 - r_i^2\right) \sigma} \tag{27}$$

The approximation z_∞ for the impedance at high frequencies is given as a function of the complex depth p :

$$z_\infty = \frac{1}{2\,\pi\,\sigma\,r_e\;p} \tag{28}$$

The derivative of the internal impedance with respect to *s* is given by:

$$\frac{dz_i}{ds} = \frac{z_\infty^2}{2\, s\, z_i} \tag{29}$$

The matrix $\mathbf{Z^{(g)}}$ containing the correction due to the finite conductivity of the ground return path can be obtained from the Carson formulas [14]. The Carson integrals can be solved by series. This approach would yield large expressions for the derivatives with respect to *s*. A simpler model that leads to good results and is used in this paper utilizes the concept of the complex depth for the ground return [15]. The ground return path correction terms obtained by this method can be added to the external impedance, as shown below:

$$z_{i,i}^{(e,g)} = z_{i,i}^{(e)} + z_{i,i}^{(g)} = s\,\frac{\mu_0}{2\,\pi}\ln\left[\frac{2\,(h_i + p)}{r_e}\right] \tag{30}$$

$$z_{i,j}^{(e,g)} = z_{i,j}^{(e)} + z_{i,j}^{(g)} = s\,\frac{\mu_0}{2\,\pi}\ln\left[\frac{\sqrt{(h_i + h_j + 2p)^2 + d_{i,j}^2}}{\sqrt{(h_i - h_j)^2 + d_{i,j}^2}}\right] \tag{31}$$

where *p* is the complex depth given in (25) with σ equal to the earth conductivity. The earth electric permittivity ε can also be included using (32).

$$p = \frac{1}{\sqrt{s\cdot\mu_0\cdot(\sigma + s\,\varepsilon)}} \tag{32}$$

The derivatives of these impedances with respect to *s* are given by:

$$\frac{d\, z_{i,i}^{(e,g)}}{ds} = \frac{z_{i,i}^{(e,g)}}{s} + \frac{s\mu_0 r_e}{4\,\pi\,(h_i + p)}\frac{dp}{ds} \tag{33}$$

$$\frac{d\, z_{i,j}^{(e,g)}}{ds} = \frac{z_{i,j}^{(e,g)}}{s} + \frac{s2\mu_0}{\pi}\frac{\sqrt{(h_i - h_j)^2 + d_{i,j}^2}\,(h_i + h_j + 2p)}{\sqrt{(h_i + h_j + 2p)^2 + d_{i,j}^2}}\frac{dp}{ds} \tag{34}$$

where: $\frac{dp}{ds} = -\frac{p}{2s}$, when neglecting ε in (32).

The equivalent homopolar and non-homopolar parameters Z_u and Y_u can be obtained from reductions in the line parameter matrices, as described in [11]. The matrix derivatives with respect to *s* are obtained utilizing the derivative rules to the expressions produced during this matrix reduction.

In case the homopolar and non-homopolar modes are considered modes or quasi-modes, there exist several formulas, which allow the approximate computation of these parameters [8,11]. These formulas allow a deeper understanding of how the line parameters change with the geometrical configuration, require less data and lead to an easier computational implementation. The homopolar and non-homopolar capacitances *C* can be approximately computed from these formulas and the admittances Y_u are given by the product of *s* and the capacitances:

$$Y_{u1} = s\cdot C_1 \tag{35}$$

$$Y_{u0} = s\cdot C_0 \tag{36}$$

where indices 0 and 1 represent homopolar and non-homopolar quantities respectively.

The homopolar and non-homopolar longitudinal impedances are given by the sum of the three terms below (external, internal and ground correction impedances):

$$Z_{u1} = Z_1^{(e)} + Z_1^{(i)} + Z_1^{(g)} \tag{37}$$

$$Z_{u0} = Z_0^{(e)} + Z_0^{(i)} + Z_0^{(g)} \tag{38}$$

The external impedance is given by the product of *s* and the external inductance $L^{(e)}$, which does not depend on s:

$$Z_{u1}^{(e)} = s\cdot L_1^{(e)} \tag{39}$$

$$Z_{u0}^{(e)} = s\cdot L_0^{(e)} \tag{40}$$

The approximated formulas for the homopolar and non-homopolar external inductances can be obtained from the capacitances, based on property (22):

$$L_1^{(e)} = \frac{\mu_0\cdot\varepsilon_0}{C_1} \tag{41}$$

$$L_0^{(e)} = \frac{\mu_0\cdot\varepsilon_0}{C_0} \tag{42}$$

The internal impedance term is equal for the homopolar and non-homopolar components, and is obtained by direct division of the conductor impedance in (23) by the number of subconductors in the bundle.

$$Z_{u1}^{(i)} = Z_{u0}^{(i)} = \frac{z_i}{n_s} \tag{43}$$

where n_s is the number of subconductors in the bundle. The derivative of the internal impedance may be similarly obtained:

$$\frac{d\, Z_{u1}^{(i)}}{ds} = \frac{d\, Z_{u0}^{(i)}}{ds} = \frac{1}{n_s}\frac{dz_i}{ds} \tag{44}$$

The correction for the effects of the ground return path can be considered together with the external inductance utilizing approximate formulas based on the geometrical mean distances [8,11] considering the complex plane of the return path [15]. This is similar to the method utilized in the assembling of the impedance matrices in (30) and (31).

The lack of specific geometric information and in cases where it is acceptable an additional small error, the following approximate formulas can be used. They are valid for medium-range frequencies (up to a few kHz) for usual values of ground conductivity. These formulas, when separately considered from the external inductance, are:

$$Z_1^{(g)} = \frac{s\ \mu_0}{2\,\pi}\ln\left[\frac{(H + p)\cdot H'}{(H' + p)\cdot H}\right] = \frac{s\ \mu_0}{2\,\pi}\ln\left[\frac{1 + \frac{p}{H}}{1 + \frac{p}{H'}}\right] \tag{45}$$

$$Z_0^{(g)} = \frac{s\ \mu_0}{2\,\pi}\ln\left[\frac{(H + p)\cdot(H' + p)^{(nf-1)}}{H\cdot H'^{(nf-1)}}\right] = \frac{s\ \mu_0}{2\,\pi}\ln\left[\left(1 + \frac{p}{H}\right)\cdot\left(1 + \frac{p}{H'}\right)^{(nf-1)}\right] \tag{46}$$

where *nf* is the number of phases in the line, *H* is twice the value of the geometric mean height of the conductors and *H′* the geometric mean distance between the conductors and their mirror images reflected in the ground

plane. The distances H and H' may be utilized as adjustable parameters in the model. These parameters are adjusted such that the line behavior may be better represented as a function of frequency.

VI. RESULTS

Example results will be shown considering a 300 km long, 500 kV transmission line, with the following non-homopolar parameters (positive sequence) at 60 Hz:

$$Z_u = 0.028\ \Omega/\text{km} + s \cdot 0.862\ \text{mH/km}\quad Y_u = s \cdot 0.0138\ \mu\text{F/km}$$

A line energization study was carried out, applying a sinusoidal voltage disturbance at the sending end (input variable of $G(s)$) and monitoring the voltage at the receiving end (output variable of $G(s)$), which is kept open.

The frequency response plot of $G(s)$, shown in Fig. 1, was obtained when neglecting the frequency dependency in the line parameters. Fig. 2, on the other hand, shows the same transfer function plot when the line internal impedance is modeled by Bessel functions. The internal impedance were obtained for a line model having 3 subcondutors per bundle, with 14.8 mm of external radius and 3.70 mm of internal radius.

It is clearly seen that the frequency dependency of the internal impedance caused a significant increase in the damping of the higher frequency poles. Table 1 shows the poles, computed by the dominant pole algorithm, for the two cases (considering or not the frequency dependency of the internal line impedance).

Table 1 - Comparison of Line Poles for Two Models

Poles (rad/s) (without frequency dependency)	Freq. (Hz)	Poles (rad/s) (with frequency dependency)	Freq. (Hz)
–16.241 + *j* 1518.0	242	–18.758 + *j* 1506.0	240
–16.241 + *j* 4554.3	725	–29.508 + *j* 4528.7	721
–16.241 + *j* 7590.6	1208	–37.306 + *j* 7557.5	1203
–16.241 + *j* 10626.8	1691	–43.346 + *j* 10587.6	1685

The transfer function residues associated with the line poles were also obtained and are listed in Table 2.

Table 2 - Residues of $G(s)$ for Various Poles

Poles (rad/s)	Freq. (Hz)	Residue (pu)
–18.758 + *j* 1506.0	240	+3.145 – *j* 959.96
–29.508 + *j* 4528.7	721	–2.980 + *j* 963.62
–37.306 + *j* 7557.5	1203	+2.117 – *j* 964.37
–43.346 + *j* 10587.6	1685	–1.771 + *j* 964.66

The frequency response of the reduced model incorporating the first four pairs of complex-conjugate poles is an excellent approximation of the exact $G(j\omega)$ for frequencies up to 2,000 Hz (visually coincident with Fig. 2). The frequency response of the reduced model, incorporating only the first three pairs of complex-conjugate poles (see Fig. 3) is an excellent approximation of $G(j\omega)$ for frequencies up to 1,300 Hz.

The line was energized by a 60 Hz sinusoidal signal applied to the line sending end, the Laplace transform for this signal is given by (47), where ω_s is the nominal angular frequency.

$$u(t) = \sin(\omega_s\ t) \Rightarrow U(s) = \frac{\omega_s}{s^2 + \omega_s^2} \tag{47}$$

The residues of the poles for this sinusoidal disturbance may then be obtained by multiplying the residues of the

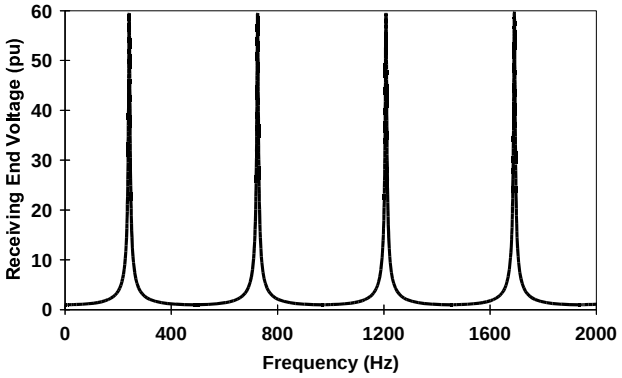

Fig. 1 - Frequency response of $G(s)$ when neglecting the frequency dependency in the line parameters.

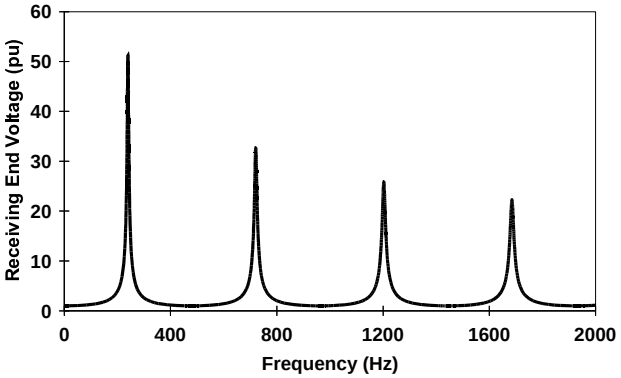

Fig. 2 - Frequency response of $G(s)$ when considering frequency dependency in the internal impedances.

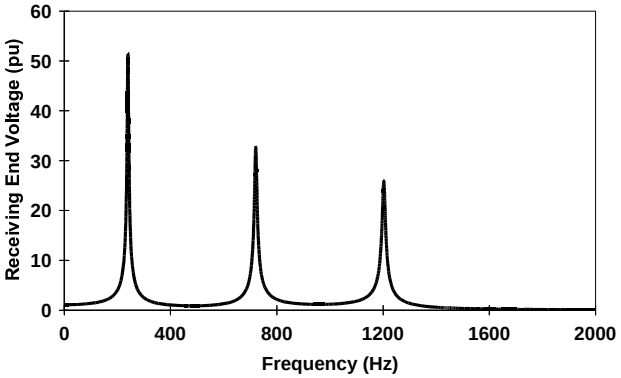

Fig. 3 - Approximate frequency response of $G(s)$ for a 6th order model of the transmission line.

transmission line transfer function (Table 2) by the Laplace transform of the sine function in (47), as shown in (48).

$$\overline{R}_i = R_i \cdot \frac{\omega_s}{\lambda_i^2 + \omega_s^2} \tag{48}$$

Table 3 shows the numerical values for the residues of the line transfer function $G(s)$ already multiplied by the sinusoidal disturbance.

Table 3 - Residues of G(s) multiplied by the sinusoidal input

Pole (rad/s)	Freq. (Hz)	Residue $\overline{R}_i$ (pu)
–18.758 + *j* 1506.0	240	+0.00396 + *j* 0.17015
–29.508 + *j* 4528.7	721	–0.00018 – *j* 0.01783
–37.306 + *j* 7557.5	1203	+0.00005 + *j* 0.00638
–43.346 + *j* 10587.6	1685	–0.00002 – *j* 0.00325

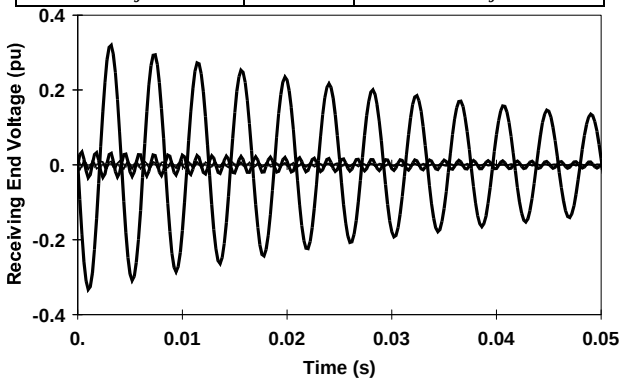

Fig. 4 - Four Individual Modal Responses

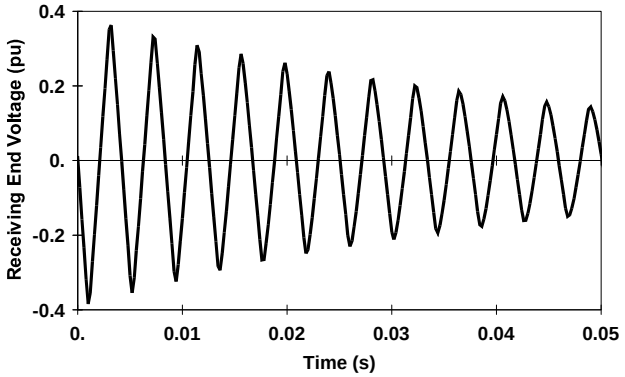

Fig. 5 - Transient response of the system

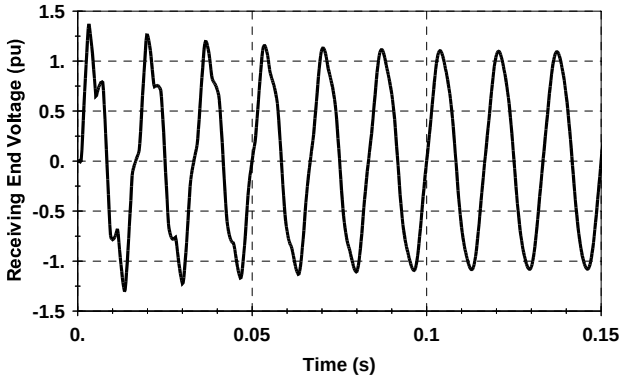

Fig 6 - Energizing receiving end voltage response

Each pole and associated residue in Table 3 produces a damped sinusoid in the time domain. Note that the higher frequency poles have smaller residues, as expected. Fig. 4 presents the four individual modal responses. The sum of these four modal responses will produce the transient response of the system, as presented in Fig. 5.

The system steady-state response is given by a sinusoidal signal of 60 Hz, whose modulus and phase are determined by the transfer function $G(j\,\omega_s)$ multiplied by the amplitude of the input. In the results below a 1 pu amplitude for the sinusoidal input was assumed:

$$G(j\,\omega_s) = 1.0827 - j\,0.00758 = 1.0827 / \underline{0.40^{\circ}}$$

The steady state overvoltage due to Ferranti effect is, then, equal to 8.27%.

The complete system response is given by the sum of the transient and steady-state components, and is shown in Fig. 6. Note the time scale of Fig. 6 (0.15 s) is different from that in Figs. 4 and 5 (0.05 s).

One should note that the initial overvoltage transients are dominated by the pole of 240 Hz and its associated residue. Modal analysis allows monitoring this residue and other sensitivities [16], to determine means to reduce transients.

VII. CONCLUSIONS

A detailed transmission lines model was developed for the modal analysis of ac networks. The frequency dependency of line parameters was considered, including skin effect and ground return. The modal analysis results clearly show the importance of considering these frequency dependent effects. The s-domain modeling approach was shown to be more suitable to the modal analysis as compared to state space or descriptor system approaches. In these last two approaches, the frequency dependency and the distributed nature of the line parameters may be only approximately modeled.

VIII. REFERENCES

[1] H. W. Dommel, "Digital Computer Solution of Electromagnetic Transients in Single and Multiphase Networks", *IEEE Transactions on Power App and Systems*, vol. PAS 88, no. 4, April 1969, pp. 388-399.

[2] W. S. Meyer, H. W. Dommel, "Numerical Modeling of Frequency-Dependent Transmission Line Parameters in a Electromagnetic Transients Program", *IEEE Transactions on Power App and Systems*, vol. PAS 93, no. 4, Sept-Oct. 1974, pp. 1401-1409.

[3] J. R. Marti, "Accurate Modeling of Frequency-Dependent Transmission Lines in Electromagnetic Transient Simulations", *IEEE Transactions on Power App and Systems*, vol. PAS 101, no. 1, January 1982, pp. 147-155.

[4] P. M. Anderson, B. L. Agrawal, J. E. Van Ness, *Subsynchronous Resonance in Power System* , IEEE Press, New York.

[5] L. T. G. Lima, N. Martins, S. Carneiro Jr., "Augmented State-Space Modeling of Large Scale Linear Networks", *Proceedings of the IPST'99 - International Conference on Power System Transients*, Budapest, Hungary, June 1999.

[6] A. Semlyen, "s-Domain Methodology for Assessing the Small Signal Stability of Complex Systems in Non-Sinusoidal Steady State", *IEEE Transactions on Power Systems*, vol. 6, no. 1, February 1999, pp. 132-137.

[7] S. Gomes Jr., N. Martins, C. Portela, "Modal Analysis Applied to s-Domain Models of ac Networks", *Procedings of the IEEE/PES Winter Meeting*, Columbus, Ohio, January 2001.

[8] W. D. Stevenson Jr., *Elements of Power System Analysis*, 4th ed., Mc Graw Hill, 1982.

[9] G. H. Golub, C. F. Van Loan, *Matrix Computation*, The Johns Hopkins University Press, 1989.

[10] L. T. G. Lima, *Descriptor System Approach for Transient Analysis of Large Scale Power Systems*, Ph.D. Thesis, COPPE/UFRJ, Rio de Janeiro, Brazil, March 1999 (in Portuguese)

[11] P. M. Anderson, *Analysis of Falted Power Systems*, Iowa University Press, Iowa.

[12] H. B. Dwight, "Skin Effect in Tubular and Flat Conductors", *AIEE Transactions*, vol. 37, pt. II, 1918, pp. 1379-1403.

[13] A. Semlyen, A. Deri, "Time Domain Modeling of Frequency Dependent Three-Phase Transmission Line Impedance", *IEEE*

Transactions on Power App. and Systems, vol. PAS-104, June 1985, pp. 1549-55.

[14] J. R. Carson, "Wave Propagation in Overhead Wires with Ground Return", *Bell System Technical Journal*, vol. 5, 1926.

[15] A. Deri, G. Tevan, A. Semlyen, A. Castanheira, "The Complex Ground Return Plane: A Simplified Model for Homogeneous and Multi-Layer Earth Return", *IEEE Transactions on Power App. and Systems*, vol. PAS-100, August 1981, pp. 3686-93.

[16] S. L. Varricchio, S. Gomes Jr., N. Martins, "s-Domain Approach to Reduce Harmonic Voltage Distortions Using Sensitivity Analysis", *Procedings of the IEEE/PES Winter Meeting*, Columbus, Ohio, January 2001.